I J C T A, 9(8), 2016, pp. 3415-3422

PANDA ring resonator for optical Gas and Pressure sensing applications

G. Bhuvaneswari*, D. Shanmuga sundar* and A. Sivanantha Raja*

ABSTRACT

A new system of microring sensing transducer using a PANDA ring resonator type, in which the sensing unit is consisted of an optical add/drop filter and two nanoring resonators, one of the rings is placed as a transducer (sensing unit), while the other ring is set as a reference ring is proposed. The panda ring resonator works on the principle of interferometric concept which can be used for various sensing applications. Panda ring resonator based gas sensor is designed for various gases such as chloroform, ammonia, benzene which are used in real time applications and the performance of the systems for different gases with different split rings were analyzed. The efficiency of the system is increased by increasing the number of split rings. For pressure sensor, the external force is assumed to exert on the sensing ring resonator. Finite difference time domain (FDTD) method via the computer programming called Optiwave is used to simulate the sensing behaviors. The obtained results have shown that the change in wavelength at the sensing unit due to the change in sensing ring is seen. Within a PANDA ring resonator, the behavior of light is also analyzed.

Keywords: PANDA ring resonator, split gaps, external force

1. INTRODUCTION

NOW a days, the micro-resonator [1, 2] and the sensor based on the integrated optical finds application in various fields [3, 4]. In this paper, a new sensor system for measuring various gaseous compounds and pressure is designed using a structure called an integrated nonlinear optical PANDA ring resonator which described by Yupapin et al. [5-8]. The gas sensor based on integrated optical device has been interested for its nano scale measurement [9-14]. By means of this more efficiency can be obtained.

The modified nonlinear microring resonator device, which is made up of linear optical add/drop filter incorporating two nonlinear microring/nanoring on both sides of the center ring (modified add/drop filter) which is collectively called as the PANDA ring resonator.

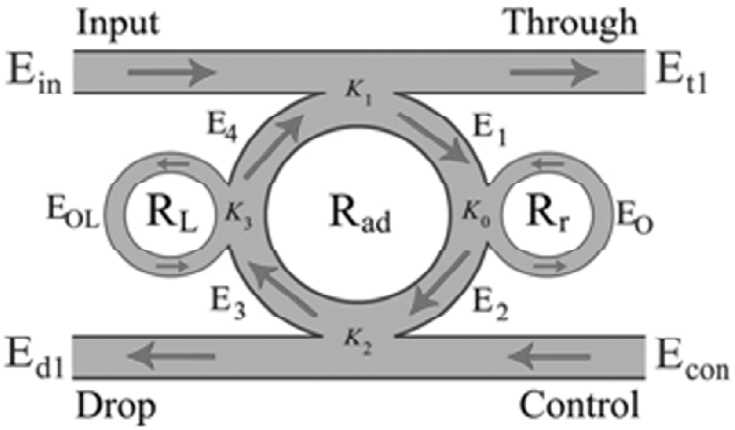

Figure 1: Schematic diagram of PANDA ring resonator

* Alagappa Chettiar College of Engineering and Technology, Karaikudi-3, *Email: Ecebhuvana45@gmail.com*

The input optical field $E_{(in)}$ of the dark soliton pulse input and the add optical field and the $E_{(control)}$ of the bright soliton or Gaussian pulse at control port are given by

$$E_{(in)}(t) = A \tan h\left[\frac{T}{T_0}\right]\exp\left[\left(\frac{z}{(2L_D)}\right) - i\omega_0 t\right]$$

$$E_{(control)}(t) = A \sec h\left[\frac{T}{T_0}\right]\exp\left[\left(\frac{z}{(2L_D)}\right) - i\omega_0 t\right]$$

$$E_{(control)}(t) = E_0 \exp\left[\left(\frac{z}{(2L_D)}\right) - i\right] \quad (1)$$

where A and z are the optical field amplitude and propagation distance, respectively. T is a soliton pulse propagation time in a frame moving at the group velocity, $T = t - \beta_1 z$, where β_1 and β_2 are the coefficients of the linear and second-order terms of Taylor expansion of the propagation constant. $L_D = T_0^2/|\beta_2|$ is the dispersion length of the soliton pulse. T_0 in equation is a soliton pulse propagation time at initial input (or soliton pulse width), where t is the soliton phase shift time, and the frequency shift of the soliton is ω_0. This solution describes a pulse that keeps its temporal width invariance as it propagates, and thus is called a temporal soliton. When a soliton of peak intensity is $|\beta_2/\Gamma T_0^2|$ given, then T_0 is known. For the soliton pulse in the microring device, a balance should be achieved between the dispersion length (L_D) and the nonlinear length ($L_{NL} = 1/\Gamma.\phi_{NL}$). Here $\Gamma = n_2 k_0$, is the length scale over which dispersive or nonlinear effects makes the beam become wider or narrower. For a soliton pulse, there is a balance between dispersion and nonlinear lengths. Hence $L_D = L_{NL}$. For Gaussian pulse in Eq. (1), E_0 is the amplitude of optical field. When light propagates within the nonlinear medium, the refractive index (n) of light within the medium is given by,

$$n = n_0 + n_2 I = \frac{n_0}{A_{eff}} \quad (2)$$

with n_0 and n_2 as the linear and nonlinear refractive indexes, respectively. I and P are the optical intensity and optical power, respectively. The effective mode core area of the device is given by A_{eff}. For the add/drop optical filter design, the effective mode core areas range from 0.1 to 0.50 μm^2, in which the parameters were obtained by using the related practical material parameters (In GaAsP/InP). When a dark soliton pulse is input and propagated within a add/drop optical filter as shown in Fig. 1, the resonant output is formed. Thus, the normalized output of the light field is defined as the ratio between the output and input fields [$E_{(out)}(t)$ and $E_{(in)}(t)$] in each roundtrip. This is given as

$$\left|\frac{E_{(out)}(t)}{E_{(in)}(t)}\right|^2 = (1-\gamma)\left[1 - \frac{\left(1-(1-\gamma)x^2\right)k}{\left(\left(1-x\sqrt{1-\gamma}\sqrt{1-k}\right)^2 + 4x\sqrt{1-\gamma}\sqrt{1-k\sin^2\left(\frac{\varphi}{2}\right)}\right)}\right] \quad (3)$$

The close form of Eqn. (3) indicates that a ring resonator in this particular case is very similar to a Fabry–Perot cavity, which has an input and output mirror with a field reflectivity, (1-k), and a fully reflecting mirror. N is the coupling coefficient, and $x = \exp(-\alpha L/2)$ represents a roundtrip loss coefficient, $\phi_0 = kLn_0$ and $\phi_{NL} = kLn_2|Ein|^2$ are the linear and nonlinear phase shifts, $k = 2\pi/\lambda$ is the wave propagation number in a vacuum. L and α are the waveguide length and linear absorption coefficient, respectively.

The optical circuits of ring-resonator add/drop filters for the through port and drop port can be given by below Eqs.

$$\left|\frac{E_t}{E_{(in)}}\right|^2 = \left(\frac{(1-k_1)-2\sqrt{(1-k_1)}\sqrt{(1-k_2)}e^{(-\alpha L/2)}\cos(k_n L)+(1-k_2)e^{-\alpha L}}{\left(1+(1-k_1)(1-k_2)e^{-\alpha L}-2\sqrt{(1-k_1)}\sqrt{(1-k_2)}e^{(-\alpha L/2)}\cos(k_n L)\right)}\right) \tag{4}$$

$$\left|\frac{E_d}{E_{(in)}}\right|^2 = \frac{k_1 k_2 e^{\left(-\alpha L/2\right)}}{\left(1+(1-k_1)(1-k_2)e^{-\alpha L}-2\sqrt{(1-k_1)}\sqrt{(1-k_2)}e^{\left(-\alpha L/2\right)}\cos(k_n L)\right)} \tag{5}$$

Here E_t and E_d represent the optical fields of the through port and drop ports, respectively. n_{eff} is the effective refractive index of the waveguide, and the circumference of the ring is $L = 2\pi R$, with R as the radius of the ring. The chaotic noise cancellation can be managed by using the specific parameters of the add/drop device, and the required signals can be retrieved by the specific users. k_1 and k_2 are the coupling coefficients of the add/drop filters, $k_n = 2\pi/\lambda$ is the wave propagation number for in a vacuum, and the waveguide (ring resonator) loss is $\alpha = 0.5$ dBmm^{-1}. The fractional coupler intensity loss is $\gamma = 0.1$. In the case of the add/drop device, the nonlinear refractive index is neglected.

The power output at the through port is written as

$$P_{t_1} = \left|E_{t_1}\right|^2 \tag{6}$$

The power output at the drop port is written as

$$P_{t_2} = \left|E_{t_2}\right|^2 \tag{7}$$

In this paper, a new system of optical gas and pressure sensor is designed using PANDA ring resonator device which comes under the optical integrated devices. By means of this more sensitive sensing system can be made.

2. SYSTEM DESIGN

2.1. Gas Sensor

The structure of the sensor system consists of the modified add/drop filter known as the PANDA ring resonator. In the device, one of the ring resonator is made to have splits of two, four and six so that gas compounds could penetrate inside it and replace that section. Because of this penetration the refractive index of the cavity changes. This changes leads to the change in the phase shift of the signal which depends on the gas concentration and its refractive index.

The change of an optical path length is occurred in the same way as an interferometer System while the other ring remains constant. The sensing and the reference signal are analysed, simulated and compared by using of finite difference time domain (FDTD). The result obtained has shown that the sensor unit with six splitting gaps presents more linear relation and it is better sensing transducer than the sensor unit with two splitting gaps, where finally the use of the proposed device for gas sensor nano-scale transducer can be realized. The center ring will be made of either linear or nonlinear material whereas the side rings must be of nonlinear medium. The microring resonator of the popular material InGaAsP/InP of refractive index of $n = 3.14$ is used as the nonlinear material.

The system having three micro ring resonators, the first ring is set as the reference unit and the second ring is set as the sensing unit in which the radius of the ring is split for two, four and six gaps, so that some

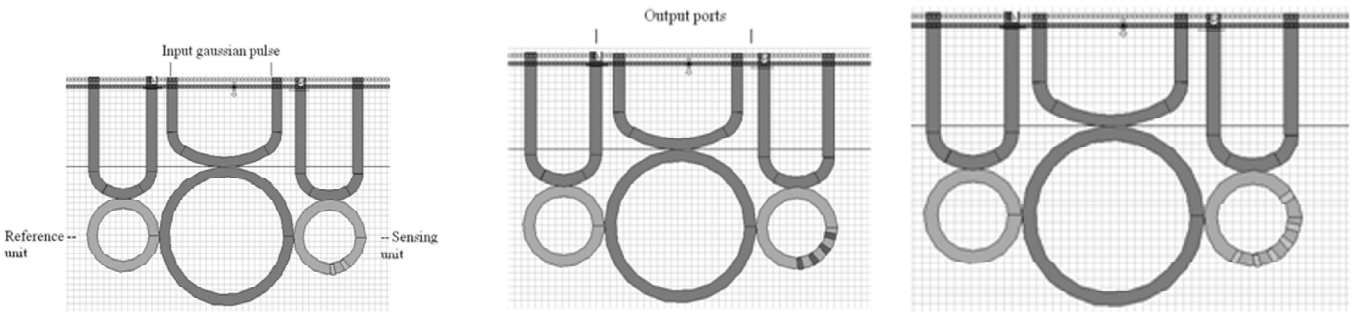

(a) **(b)** **(c)**

Figure 2: Schematic diagram of a Gas sensor using PANDA type ring resonator: (a) the sensor unit with two splitting gaps; (b) the sensor unit with four splitting gaps; (c) the sensor unit with six splitting gaps

of the gas can be penetrated between the small sections of the ring causing the change in the refractive index. Finally the third ring is referred as the interferometer and it is located at the center of the system. The radius of center ring is 1.565μm while the radius of side rings are 0.775μm. Two identical beams of Gaussian pulse of width 1550nm are launched into the system at the input port and the add port.

According to the various gaseous compounds, refractive index of the split gaps in the sensing unit can be varied. With respect to the change in refractive indices corresponding wavelength shift in the sensing unit can be analysed and measured.

2.2. Pressure Sensor

The system consisted of three microring resonators, where the first ring is position as a reference ring, with radius. The second ring is the sensing ring, the radius is varied from1.550–1.558μm and the third ring is used to form the interference signal between reference and sensing rings, with the radius 3.10μm. In operation, the change in sensing ring radius is caused the change in the shift in signals circulated in the interferometer ring, in which the interference signals are seen. The change in optical path length which is related to the change of the external parameters is measured. According to the applied force, which is exerted into the sensing ring by molecules/particles with appreciate sizes, in which the ring shape will be deformed. Hence, the shapes of the ring are deformed into an ellipse and then induced the ring circumference-shift. The sensing ring will be only immerged in the sensing media and disturbed by molecules/atoms side by side.

3. RESULTS

3.1. Analyser Output

The analyser output shows the wave propagation through the reference unit and the sensing unit with the inputs at the input port and the add port.

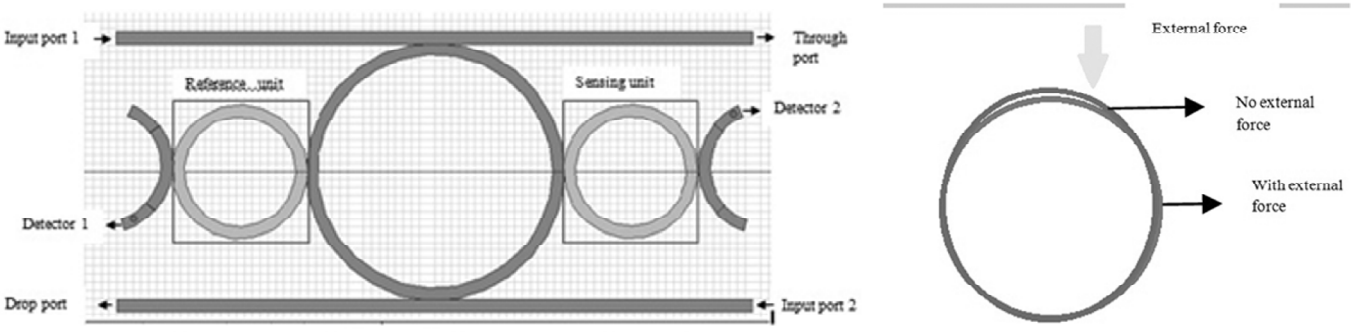

(a) **(b)**

Figure 3: (a) Schematic diagram of a nanoscale sensing transducer using a PANDA ring resonator. (b) Deformation shape of sensing ring within the Sensing Unit with and without external force.

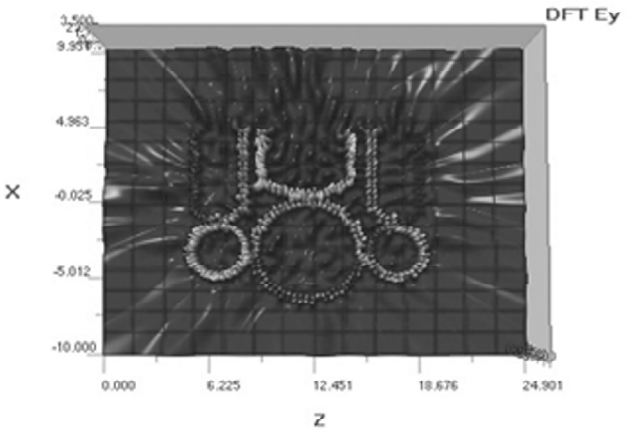

Figure 4: Analyser output of PANDA ring resonator with interferometric concept

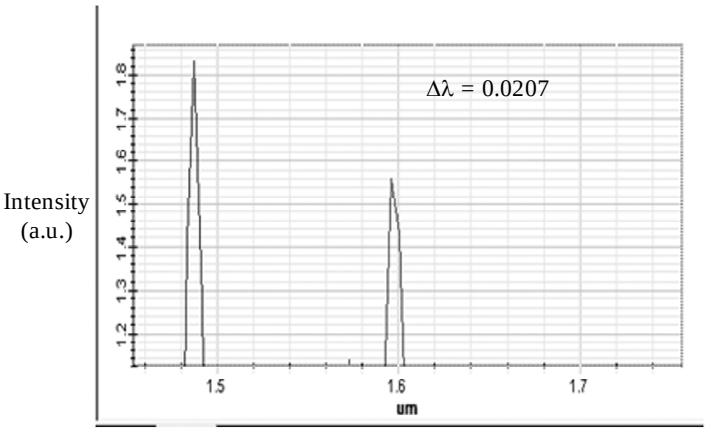

Wavelength (μm)

Figure 5: Wavelength shift for two split gaps with *n* = 1.50

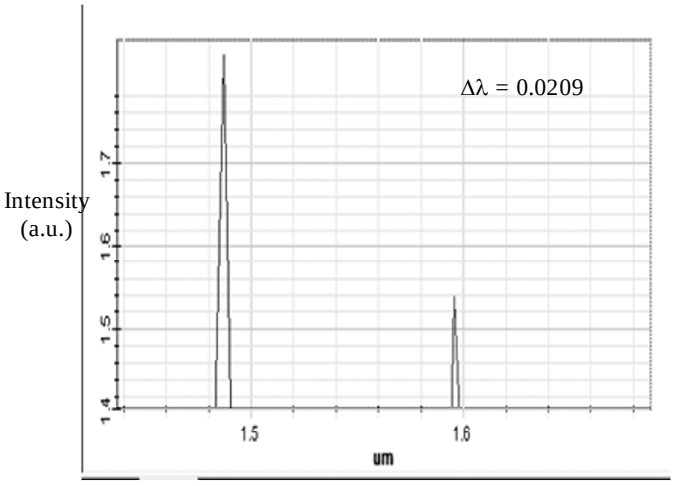

Wavelength (μm)

Figure 6: Wavelength shift for four split gaps with *n* = 1.50

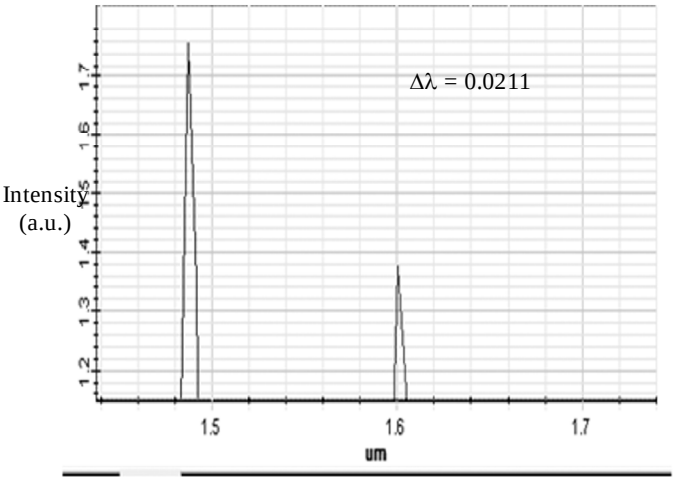

Wavelength (μm)

Figure.7 Wavelength shift for six split gaps with *n* = 1.50

In the above graph, black curve represents the reference signal and blue curve represents the sensing signal. The above graphs shows that the increase in the number of split gaps in the sensing unit increases the amount of wavelength shift. In the analyzer output, the difference between the center wavelength of reference signal and the sensing signal at the detector port leads to the wavelength shift. Thus the more linear measurement resolution can be found with the increase in the split gaps.

The tabulation predicts the relation between the various refractive indices and its corresponding wavelength shift for various split gaps in the sensing unit. The sensing application can also be extended to the real time gases for various applications like safety purpose etc., From that it is found more clearly that measurement accuracy will be greater in the increased split gaps and also the shift will be more while increasing the refractive index values.

R.I–Refractive Index. This representation shows that the linear relation between the wavelength shift and the refractive index will be more when the number of splitting gap increases. Thus results obtained have shown that the sensing system with more gap have better measurement resolution than the sensing system with less gap. The advantage is that remote measurement is also available due to the use of the integrated optic link.

Table 1
Relation Between The Refractive Index and The Wavelenth Shift for Various Split Gaps

No. of split gap / n	2	4	6
1.5	0.0207	0.0208	0.0360
1.6	0.0209	0.0225	0.0364
1.7	0.0211	0.0233	0.0369

Table 2
Change of Wavelength Shift for Real Time Gases

No. of split gap / n	2	4	6
AIR 1.000 292	0.013361	0.03257	0.045002
AMMONIA 1.000 444	0.02650	0.056985	0.08576
BENZENE 1.000 762	0.050445	0.058952	0.102816
CHLOROFORM 1.001 450	0.057919	0.0599413	0.102933

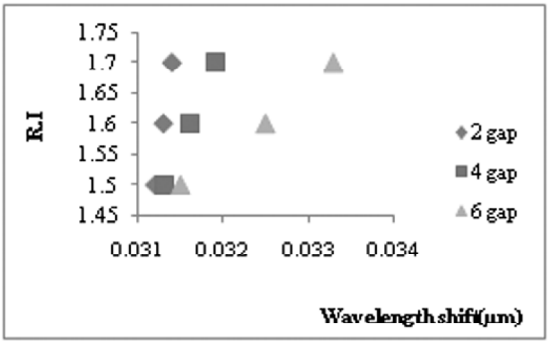

Figure 8: Relation between wavelength shift and the refractive index for various split gaps

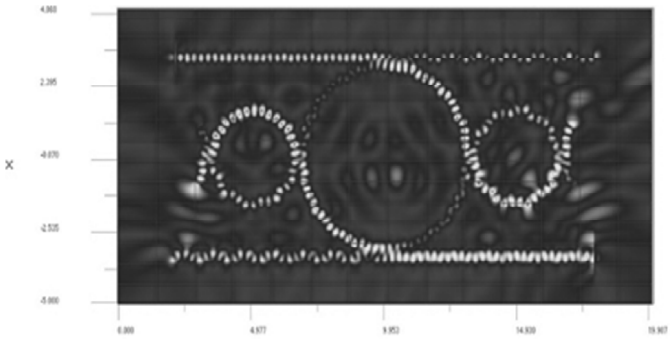

Figure 9: Analyser output of pressure sensing system

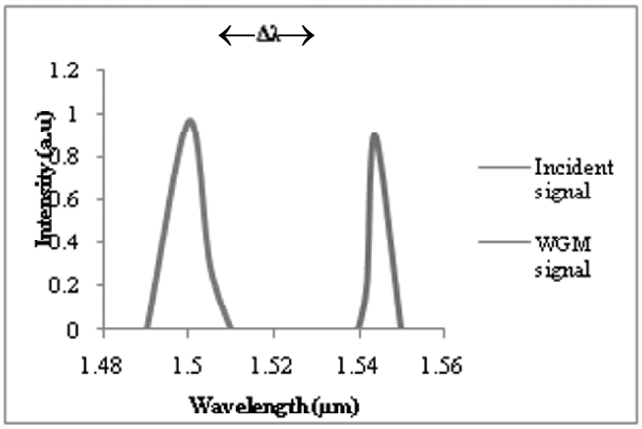

Figure 10: Shows the relationship between intensity and wavelength of sensing and reference signals, with the radius of reference unit (1.55μm) – blue curve and the radius of sensing unit (varied from 1.552 – 1.568μm) – red curve.

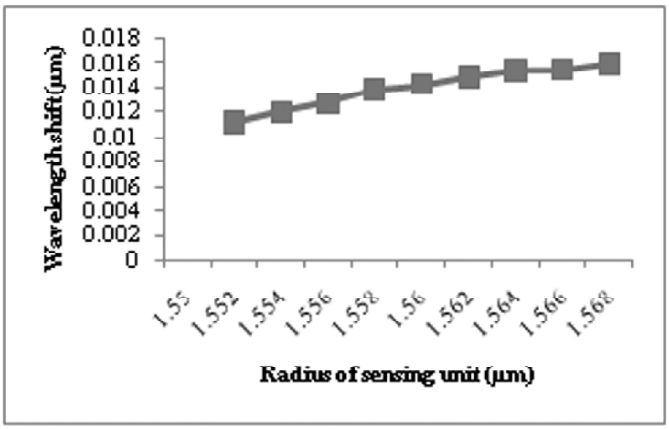

Figure 11: Graph of the linear relationship between sensing ring radius and wavelength shift of detector 2 signal

Table 3
Relationship Between Sensing Ring Radius and Wavelength Shift of Detector 2 Signal

Sensing ring radius (μm)	Wavelength shift (μm)
1.552	0.010263
1.554	0.011991
1.556	0.012695
1.558	0.013801
1.56	0.014690
1.562	0.015347
1.564	0.01590

3.2. Parameter Analysis

3.2.1. Wavelength Shift

Due to the variation in the refractive index of the split gaps, there occurs shift in the wavelength of sensing signal which may be calculated by

$$\Delta\lambda = \lambda_2 - \lambda_1 \tag{8}$$

Where λ_1 is the wavelength of reference signal and λ_2 is the wavelength of sensing signal.

3.2.2. Change in The Refractive Index Of The Cavity

According to the properties of InGaAsP/InP, the relation between refractive index and the wavelength shift can be related by the following relation

$$\Delta n = \Delta\lambda/\lambda \; . \; n_0 \tag{9}$$

Where Δn is the change in the refractive index of the cavity

n_0 is the initial refractive index of the cavity.

4. CONCLUSION

In this project, a new system of nano scale gas sensor and pressure sensor using panda type ring resonator is designed and the characteristics are analyzed. The calibration is allowed by using the change in wavelength between sensing and reference signals, which is existed within the system. Thus increasing the split rings increase the efficiency of the gas sensor and the wavelength shift for the each sensor is measured and reported. By means of this, more sensitive and accurate system was realized.

REFERENCES

[1] Y.G. Boucher, P. Feron, Generalized transfer function: a simple model applied to active single-mode, microring resonators, Opt. Commun. 282 (2009) 940-3947.

[2] Y. Dumeige, C. Arnaud, P. Feron, Combining FDTD with coupled mode theories for biostability in micro-ring resonators, Opt. Commun. 250 (2005) 376-383.

[3] N. Fabricius, G. Gauglitz, J. Ingenhoff, A gas sensor based on an integrated optical Mach-Zehnder interferometer, Sens. Actuators B: Chem. 7 (1-3 (March)) (1992) 672-676.

[4] K. Fischer, J. Müller, Sensor application of SiON integrated optical waveguides on silicon, Sens. Actuators B: Chem. 9 (3 (October)) (1992) 209-213.

[5] K. Uomwech, K. Sarapat, P.P. Yupapin, Dynamic modulated Gaussian pulse propagation within the double PANDA ring resonator, Microw. Opt. Technol. Lett. 52 (8 (August)) (2010).

[6] P.P. Yupapin, S. Suchat, Entangled photon generation using a fiber optic Mach-Zehnder interferometer incorporating the nonlinear effect in a fiber ring resonator, Nanophotonics 1 (2007) 013504.

[7] B. Piyatamrong, K. Kulsirirat, W. Techitdheera, S. Mitatha, P.P. Yupapin, Dynamic potential well generation and control using double resonators incorporating in an add/drop filter, Mod. Phys. Lett. B 24 (32) (2010) 1-9.

[8] T. Phatharaworamet, Chat Teeka, R. Jomtarak, S. Mitatha, P.P. Yupapin, Random binary code generation using dark-bright soliton conversion control within a PANDA ring resonator, IEEE J. Lightwave Technol. 28 (19) (2010) 2804-2809.

[9] G. Yang, I.M. White, X. Fan, An opto-fluidic ring resonator biosensor for the detection of organophosphorus pesticides, Sens. Actuators B 133 (2008) 105-112.

[10] D. Tang, D. Yang, Y. Jiang, J. Zhao, H. Wangc, S. Jiang, Fiber loop ring-down optical fiber grating gas pressure sensor, Opt. Lasers Eng. 48 (2010) 1262-1265.

[11] G.Z. Xiao, A. Adnet, Z. Zhang, F.G. Sun, C.P. Grover, Monitoring changes in the refractive index of gases by means of a fiber optic Fabry-Perot interferometer sensor, Sens. Actuators A 118 (2005) 177-182.

[12] S.M. Murtry, J.D. Wright, D.A. Jackson, Sensing applications of a low-coherence fibre-optic interferometer measuring the refractive index of air, Sens. Actuators B 72 (2001) 69-74.

[13] S. Punthawanunt, S. Songmuang, S. Mitatha and P.P. Yupapin, Dynamic Optical Tweezers Generation using a PANDA Ring Resonator, Procedia Engineering 8 (2011) 467-473.

[14] Kreangsak Tamee, Keerayoot Srinuanjan, Somsak Mitatha, and Preecha P. Yupapin, Distributed Sensors Using a PANDA Ring Resonator Type in Multiwave length Router, IEEE Sensors Journal, Vol. 11, No. 9, September 2011 1987.